

The effect of cyclic mechanical strain on the expression of adhesion-related genes by periodontal ligament cells in two-dimensional culture

A. Saminathan¹, K. J. Vinoth¹,
D. C. Wescott², M. N. Pinkerton²,
T. J. Milne², T. Cao¹, M. C. Meikle¹

¹Faculty of Dentistry, National University of Singapore, Singapore and ²Department of Oral Sciences, Faculty of Dentistry, University of Otago, Dunedin, New Zealand

Saminathan A, Vinoth KJ, Wescott DC, Pinkerton MN, Milne TJ, Cao T, Meikle MC. The effect of cyclic mechanical strain on the expression of adhesion-related genes by periodontal ligament cells in two-dimensional culture. *J Periodont Res* 2012; 47: 212–221. © 2011 John Wiley & Sons A/S

Background and Objective: Cell adhesion plays important roles in maintaining the structural integrity of connective tissues and sensing changes in the biomechanical environment of cells. The objective of the present investigation was to extend our understanding of the effect of cyclic mechanical strain on the expression of adhesion-related genes by human periodontal ligament cells.

Material and Methods: Cultured periodontal ligament cells were subjected to a cyclic in-plane tensile deformation of 12% for 5 s (0.2 Hz) every 90 s for 6–24 h in a Flexercell FX-4000 Strain Unit. The following parameters were measured: (i) cell viability by the MTT assay; (ii) caspase-3 and -7 activity; and (iii) the expression of 84 genes encoding adhesion-related molecules using real-time RT-PCR microarrays.

Results: Mechanical stress reduced the metabolic activity of deformed cells at 6 h, and caspase-3 and -7 activity at 6 and 12 h. Seventy-three genes were detected at critical threshold values < 35. Fifteen showed a significant change in relative expression: five cell adhesion molecules (*ICAM1*, *ITGA3*, *ITGA6*, *ITGA8* and *NCAM1*), three collagen α -chains (*COL6A1*, *COL8A1* and *COL11A1*), four MMPs (*ADAMTS1*, *MMP8*, *MMP11* and *MMP15*), plus *CTGF*, *SPP1* and *VTN*. Four genes were upregulated (*ADAMTS1*, *CTGF*, *ICAM1* and *SPP1*) and 11 downregulated, with the range extending from a 1.76-fold induction of *SPP1* at 12 h to a 2.49-fold downregulation of *COL11A1* at 24 h.

Conclusion: The study has identified several mechanoresponsive adhesion-related genes, and shown that onset of mechanical stress was followed by a transient reduction in overall cellular activity, including the expression of two apoptosis 'executioner' caspases.

Murray C. Meikle, Faculty of Dentistry, National University of Singapore, 11 Lower Kent Ridge Road, Singapore 119083
Tel: +65 6772 6840
Fax: + 65 6773 2602
e-mail: pndmcm@nus.edu.sg

Key words: adhesion-related gene; apoptosis; cyclic mechanical strain; periodontal ligament cell; real-time RT-PCR microarray

Accepted for publication September 2, 2011

The periodontal ligament is a specialized connective tissue that has evolved to provide attachment of teeth to the

bone of the jaws. The periodontal ligament functions in a mechanically active environment and, in addition to

its attachment role, serves as a shock absorber to protect the tooth-supporting alveolar bone from excessive

occlusal loading, not only during mastication, deglutition and speech, but also due to occlusal trauma and man-made orthodontic appliances.

Numerous *in vitro* studies have investigated the effects of cyclic and continuous mechanical strain on gene expression by human periodontal ligament cells. Most have focused on alterations in the expression of a small number of cytokine and osteogenic genes (1–4), but microarrays which allow the activity of numerous genes to be monitored simultaneously have also been reported (5–8). Alterations in cell–matrix and cell–cell adhesion play important roles not only in maintaining the structural integrity of connective tissues, but also in sensing changes in the biomechanical environment of cells and mediating the transmission of bidirectional forces across their plasma membranes (9–11). Periodontal ligament cells, derived as they are from a biomechanically active tissue, therefore offer an excellent experimental model for investigating the expression of genes involved in these interactions.

All cells have a finite life span, and apoptosis, a form of programmed cell death in which cells are induced to activate their own death or suicide, plays an important role in many pathophysiological processes, including tissue remodelling and homeostasis (12,13). However, cultured bone and periodontal ligament cells deprived of the normal functional loading to which they are exposed *in vivo* are in a physiological default state, raising the question of what effect mechanical stimuli might have on apoptosis-mediated cell death. The *in vitro* evidence to date is equivocal. Although complicated by the use of different model systems and strain regimens, unlike cultured bone cells, where mechanical stimuli have typically been shown to inhibit apoptosis (14,15), in cultured human periodontal ligament cells cyclic mechanical strain has been reported to trigger a transient increase in apoptosis (16,17). This is important because any reductions in metabolic activity may compromise quantification of alterations in gene expression.

In the present investigation, human periodontal ligament cells in two-

dimensional culture were screened for adhesion-related genes using targeted real-time RT-PCR microarrays, and we report, for the first time, the effect that a predominantly tensile cyclic mechanical strain has on their expression. We further show that the immediate response of the cells to a change in their biophysical environment was a short-term reduction in overall cellular activity, including the expression of two apoptosis 'executioner' caspases.

Material and methods

Preparation of human periodontal ligament cells

Premolar teeth that had been extracted for orthodontic reasons were used to establish human periodontal ligament cell cultures as described previously (18). Approval to harvest human tissue from extracted teeth with the consent of the donor and/or parent was granted by the Ethics Committees of the University of Otago (reference 05/069) and National University of Singapore (NUS-IRB reference 08-015). Teeth were washed with phosphate-buffered saline and fragments of the periodontal ligament attached to the middle third of the root removed with a scalpel. Tissue explants were plated onto 3 cm Petri dishes in Dulbecco's modified Eagle's medium (Gibco, Invitrogen, Auckland, NZ, USA) supplemented with 10% fetal calf serum (Gibco) and antibiotic–antimycotic reagent (10,000 units penicillin, 10,000 µg streptomycin and 25 µg/mL amphotericin B; Invitrogen), 100 mmol L-glutamine (Invitrogen) and gentamicin (10 mg/mL; Gibco) and cultured at 37°C in a humidified atmosphere of 5% CO₂–95% air. On reaching confluence, the cells were lifted with trypsin–EDTA (Gibco) and serially passaged through 25, 75 and 175 cm² tissue culture flasks (Cellstar; Greiner Bio-One AG, Munroe, NC, USA). Passage two cells were frozen in Cell Culture Freezing Medium (Gibco) at –80°C and transferred to liquid nitrogen for long-term storage. Third or fourth passage cells were used for experimental purposes.

Application of cyclic mechanical strain to periodontal ligament cells

Human periodontal ligament cells (3×10^5 per well) were subcultured into six-well, 35 mm flexible-bottomed UniFlex[®] Series culture plates containing a centrally located rectangular strip (15.25 × 24.18 mm) coated with type I collagen. When the cells had reached confluence (commonly 3–4 d), the silicon rubber membranes were subjected to an in-plane deformation of 12% for 5 s (0.2 Hz) every 90 s using a square waveform, around rectangular ArcTangle[™] loading posts (required to correctly apply uniaxial strain to the cells) in a standard Bioflex baseplate linked to a Flexercell FX-4000 strain unit (Flexcell Corp., Hillsborough, NC, USA). The strain value of 12% was based on data derived from a finite element model, which suggested that maximal periodontal ligament strains for horizontal displacements of a human maxillary central incisor under physiological loading lies in the vicinity of 8–25%, depending upon the apico-crestal position. Deformation of 12% correlates well with strain conditions predicted at the mid-root (19). Experimental and control plates were allocated to each of the three time points (6, 12 and 24 h) and separate experiments performed for light microscopy, cell activation, caspase activity and RNA extraction. As discussed in detail later, the deformation of the silicon membrane is not uniform, but generates a tension gradient; any changes in expression will therefore represent the global average of cells exposed to different amounts of strain.

Changes in cell morphology

At the end of the experimental period, plates were examined by light microscopy to determine changes in the orientation of the cells and evidence of cellular detachment or collagen delamination. Some cultures were fixed with acetic methanol (one part glacial acetic acid; three parts methanol) for 5 min at 25°C and, after aspirating the fixative, 1% Giemsa stain (G9641; Sigma-Aldrich, Singapore) in acetic

methanol was added for 2–5 min at 25°C. After washing with 60% methanol in water for 1–2 min, rectangular segments were cut from the silicon membranes and, after mounting on glass slides, viewed by light microscopy.

MTT assay for cell viability

Cell activation was measured by the MTT assay (Sigma-Aldrich), a colorimetric assay for estimating mammalian cell survival, proliferation and activation based on the ability of viable cells to reduce yellow 3-(4, 5-dimethylthiazol-2-yl)-2, 5-diphenyl tetrazolium bromide (MTT) by mitochondrial succinate dehydrogenase (20,21). At the end of each time point the cells were harvested by trypsinization and resuspended in fresh media; 50 μ L of this cell suspension was added to 96-well plates and spun at 1800 *g* for 5 min. The supernatant was removed and 50 μ L of the MTT solution (4 mg/mL in Dulbecco's modified Eagle's medium) added to each well. The cells were incubated at 37°C for 2 h in the dark. Following incubation, the plate was centrifuged and the supernatant discarded. The resulting formazan crystals were dissolved by the addition of 200 μ L of dimethylsulfoxide (Sigma-Aldrich), and absorbance was measured at 570 nm in a microplate reader (Tecan SpectrophorPlus, Singapore).

Caspase-3 and -7 assay

Caspases, a family of cysteine proteinases that specifically cleave proteins following aspartate residues, play key roles in mammalian apoptosis. Two 'executioner' caspases (3 and 7) were measured by the Caspase-Glo 3/7 Assay (Promega Corp., Madison, WI, USA), which provides a luminescent Caspase-3/7 substrate containing the tetrapeptide sequence (Asp-Glu-Val-Asp) in a reagent optimized for caspase activity, luciferase activity and cell lysis. At the end of each time period, the collagen-coated rectangular area was cut and treated with the Caspase-Glo[®] 3/7 reagent for 1 h in the dark at room temperature according to the manufacturer's instructions. Each

sample was aliquoted into triplicate tubes, and luminescence, expressed as relative light units (RLU), was measured with a Sirius Single Tube Luminescence (Berthold Detection Systems GmbH, Pforzheim, Germany).

Extraction of RNA

Culture media were removed from the wells and total RNA isolated by a modification of the method of Chomczynski and Sacchi (22). Briefly, 0.5 mL of TRIzol[®] reagent (Invitrogen) was added to each well of the Uniflex plate. After a 5 min incubation period, the cell lysate was added to a tube containing 0.1 mL of chloroform and shaken vigorously by hand for 15 s. A further incubation of 2–3 min at room temperature was required prior to centrifugation of the samples at 12,000*g* for 15 min at 4°C. Following centrifugation, 300 μ L of the clear aqueous phase was added to an equal volume of 70% ethanol and vortexed to disperse the precipitate. Sample purity was achieved using the Purelink Micro-to-Midi Total RNA Purification System (Invitrogen) in accordance with the manufacturer's instructions. Total RNA samples were eluted from the columns in 50 μ L of RNase-free water and stored at –80°C. The concentration and purity (based on the A260/280 absorbance ratio) of the samples was determined using a Nanodrop ND-1000 Spectrophotometer (Nanodrop Technologies, Rockland, DE, USA). This combined extraction technique yielded 180–250 ng RNA from six wells with an A260/280 value of 1.96 ± 0.07 ; an A260/280 value > 1.9 –2.0 corresponds to a pure sample free of contaminating protein (Applied Biosystems, Life Technologies Corporation, Carlsbad, CA, USA).

Real-time PCR array analysis

Total RNA samples were assessed for degradation status by denaturing agarose gel electrophoresis, prior to analysis. Contaminating genomic DNA was removed from total RNA samples by DNase I digestion prior to first strand synthesis. First strand synthesis was performed using the RT² PCR

array First Strand Kit (SABiosciences, Frederick, MD, USA). Samples were then screened for the expression of 84 genes encoding extracellular matrix and adhesion molecules using the RT² Profiler PCR Array System (SABiosciences). SABiosciences PCR arrays are sets of optimized PCR primer assays that perform gene expression analysis using the principle of real-time PCR. They achieve a multigene profiling capability similar to that of microarray or SuperArray technology by setting up multiple PCRs in a 96-well plate format. Experimental and control samples at each of the three time points were analysed in triplicate to allow for biological variation between samples and provide a statistically sound data set.

Statistical methods

Data from the viability and caspase assays are expressed as means \pm SEM. Differences between groups was determined by Student's *t*-test (two-tailed) using GRAPHPAD PRISM (GraphPad Software Inc., San Diego, CA, USA) and the level of significance set at $p < 0.05$. For the gene expression study, expression profiles of the target genes were measured relative to the mean critical threshold (C_t) values of five different calibrator genes (*GAPDH*, β 2-microglobulin, β -actin, *HPRT1* and *RPL13A*) using the $\Delta\Delta C_t$ method described by Livak and Schmittgen (23). Student's *t*-tests were used for statistical comparison of the control and experimental groups using mean C_t values derived from the triplicate samples (24).

Results

Under light microscopy, a difference in cellular orientation was observed as early as 6 h after the application of cyclic strain, with no evidence of cell detachment or plate delamination. While control cells remained randomly orientated, mechanically deformed cells had become reorientated away from the direction of the applied force, as previously reported (25,26). However, realignment of the cells was not uniform across the whole surface of the centrally located collagen strip, tending

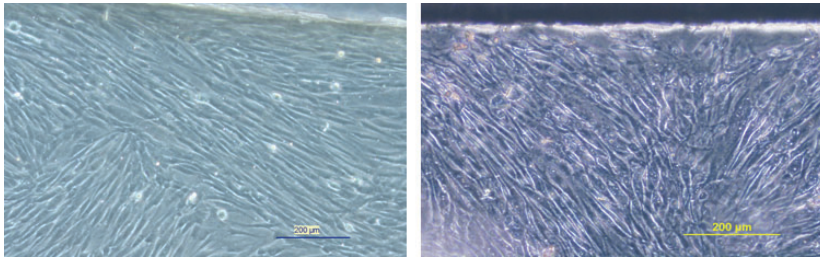


Fig. 1. The application of an in-plane deformation of 12% for 5 s (0.2 Hz) every 90 s, using a square waveform, around rectangular ArcTangle™ loading posts resulted in reorientation of the cells. Both images were taken at the edge of the centrally located type I collagen strip. Left, control culture in which cells tend to be randomly orientated. Right, 12 h stressed culture stained by the Giemsa method. Cells become aligned at varying angles to the long axis of the applied strain.

to be more pronounced towards the edges (Fig. 1).

The MTT assay showed that intermittent substrate deformation resulted in a small, but statistically significant, reduction in overall metabolic activity at 6 h (Table 1). There was also a reduction in caspase-3 and -7 activity by mechanically strained cells at 6 and 12 h, suggesting that the strain regimen had delivered a transient anti-apoptotic signal to the cells (Fig. 2).

A total of 84 cell adhesion and extracellular matrix genes were screened, and the effect of intermittent tensile strain on their differential expression is summarized in Table 2. A gene was regarded as being expressed if it was detected at a C_t value of < 35 , and using these criteria 73 genes were detectable, thereby demonstrating significant levels of basal expression. Eleven genes had C_t values ≥ 35 , which were outside the detection threshold of the system and were therefore considered not to have been expressed. This group comprised the genes for three matrix metalloproteinases (*MMP7*, *MMP9* and *MMP13*), two integrins (*ITGAL* and *ITGAM*) and three

selectins (*SELE*, *SELL* and *SELP*), plus E-cadherin (*CDH1*); Kallmann syndrome 1 sequence (*KALI*) and ϵ -sarcoglycan (*SGCE*).

Over the 24 h time course, we found statistically significant changes in the relative expression of mRNAs for 16 genes, suggesting a role for cyclic mechanical strain in regulating their function. These included six cell adhesion molecules (*ICAM1*, *ITGA3*, *ITGA6*, *ITGA8*, *ITGB1* and *NCAM1*) and three genes encoding collagen α -chains (*COL6A1*, *COL8A1* and *COL11A1*; Fig. 3); also four members of the MMP family (*ADAMTS1*, *MMP8*, *MMP11* and *MMP15*), connective tissue growth factor (*CTGF*), secreted phosphoprotein (*SPPI*; also known as bone sialoprotein/osteopontin) and the cell-attachment protein vitronectin (*VTN*; Fig. 4).

Of the mechanoresponsive genes, only four were found to be upregulated (*ADAMTS1*, *CTGF*, *ICAM1* and *SPPI*), the remaining 11 being downregulated, with the range extending from a 2.49-fold downregulation of *COL11A1* at 24 h (Fig. 3) to a 1.76-fold induction of *SPPI* at 12 h

(Fig. 4). No genes were found to be consistently up- or downregulated across all three time points, and only two [*ADAMTS1* (upregulated) and *ITGA8* (downregulated)] were expressed across two time points. Four genes (*HAS*, *ITGB4*, *LAMA2* and *TIMP3*) showed treated/control ratios of ± 2 , but none reached statistical significance ($p < 0.05$).

Discussion

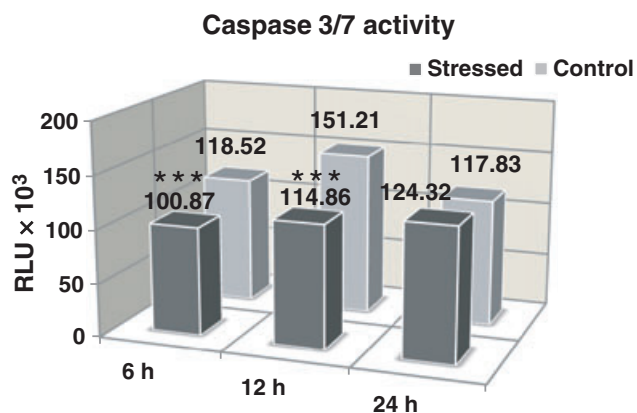
In the Flexercell™ system, a silicone membrane is stretched across a loading post by the application of vacuum pressure and, depending on the shape of the loading post, either a biaxial or a uniaxial strain (as in the present study) may be applied to the cells. Although the most widely used commercially available apparatus for delivering controlled mechanical strain to cells *in vitro*, the Flexercell system does have limitations, particularly when it comes to determining the physical characteristics of the strain. First, the mechanical in-plane deformation applied to Uniflex plates™ does not produce a purely tensional strain because tension in one plane is always accompanied by compressive and shear strains due to the Poisson effect (27,28). Second, cells cultured on a Uniflex plate will experience about half the applied substrate strain programmed into the computer (29). And third, the amount of cellular deformation will vary with the distance from the middle of the membrane; cells near the perimeter of the field will experience greater deformation (27). Nevertheless, despite the shortcomings of all existing model systems in precisely defining the strain profile, *in vitro* methodology still remains the most effective way to screen cells for the expression of mechanoresponsive genes. In any event, three-dimensional finite element analysis of the von Mises and principal stresses generated in different parts of the periodontal ligament when multirooted teeth are mechanically loaded by a masticatory force indicates that the deformation profile of the cells *in vivo* is also complex (30).

The MTT assay data, which suggested a reduction in cellular activity in mechanically deformed cultures at 6 h,

Table 1. Effect of cyclic mechanical strain on the viability of periodontal ligament cells

	6 h	12 h	24 h
Control	2.932 \pm 0.077	3.176 \pm 0.195	2.021 \pm 0.199
Stressed	2.535 \pm 0.135*	3.266 \pm 0.148	1.888 \pm 0.182

Following the application of a uniaxial, cyclic tensile strain of 12% for 5 s (0.2 Hz) every 90 s, the colorimetric MTT (tetrazolium) assay was used to detect living cells; absorbance was measured at 570 nm. Data are expressed as means \pm SEM for six wells; data are from three separate experiments. There was a small but statistically significant ($*p < 0.05$) reduction in cell viability at 6 h in mechanically stressed cultures.



	6 h	12 h	24 h
Control × 10 ³	118.52 ± 0.59	151.21 ± 0.48	117.83 ± 0.27
Stressed × 10 ³	100.87 ± 0.35	114.86 ± 0.86	124.32 ± 0.43

Fig. 2. The effect of cyclic mechanical strain on the activity of two 'executioner' caspases (caspase-3 and caspase-7) in response to a uniaxial, cyclic tensile strain of 12%. Mechanically induced strain resulted in a significant reduction in caspase activity at 6 and 12 h. Data are expressed in relative light units (RLU) as means ± SEM for six wells; data are from three separate experiments with the same batch of cells. *** $p < 0.001$.

supports the findings of a recent study using an out-of-plane, four-point bending system, which reported that a cyclic tensile strain as low as 0.5%, applied to human periodontal ligament cells for only 2 h, had an inhibitory effect on cell proliferation and viability (31). That is not to say that mechanical stress is cytotoxic, although the MTT assay is commonly used to study cytotoxicity; the signal generated in the assay is dependent upon the number and activity of living cells (20,21), but reductions in the MMT formazan product can occur without a decrease in the number of viable cells. Moreover, Wang *et al.* (31) also performed a microarray analysis using a whole-genome oligonucleotide chip and were able to identify 110 genes that were differentially expressed, 97 of which were upregulated. These data and the findings of the present study indicate that mechanically deformed cells remain metabolically active, and suggest that any changes in gene expression represent a short-term adjustment to alterations in their biophysical environment.

Our caspase-3 and -7 data suggest that the application of an in-plane cyclic strain to periodontal ligament cells has a positive, albeit transient, effect on apoptosis, an observation supported by comparable data for gingival fibroblasts

(32). It does, however, contrast with previous reports showing that an out-of-plane cyclic mechanical strain transiently increases apoptosis in periodontal ligament cells (16,17). This seems likely to have been due to the more vigorous strain regimens used (1, 10 and 20% deformation at 0.25 Hz for 10 and 6 cycles/min, respectively), suggesting that the cells might have been overstressed. Experiments conducted on human lung fibroblasts, for example, have shown that 20% cyclic deformation activated apoptotic signalling pathways (33), while 25% strain induced cell death (34). In other words, induction of apoptosis in mechanically deformed cells *in vitro* appears to be related to the magnitude and frequency of the applied strain. This is likely to be reflected in real life, where the periodontal ligament will be more heavily stressed by occlusal loading during mastication than in swallowing. The relationship between the biophysical environment of a cell and the mechanisms of programmed cell death appears to be a complicated one and would benefit from further investigation.

Cells in culture are not uniformly attached to their substrate, but are 'tack-welded' at focal adhesions, where integrin receptors physically link actin-associated cytoskeletal proteins

(talin, vinculin, α -actinin and paxillin) to the extracellular matrix (11), as well as to adhesion molecules on the surface of adjacent cells. Integrin-mediated adhesive interactions play key roles in cell migration, proliferation and differentiation, and also regulate intracellular signal transduction pathways that control adhesion-induced (outside-in) changes in cell physiology (9,10). Integrins thus function both as cell adhesion molecules and intracellular signalling receptors, and it is likely that the previously reported changes in cell signalling in response to mechanical deformation are downstream of events mediated by integrins (35). Fourteen integrin subunits were detected at C_t values < 35 , confirming previous findings that human periodontal ligament cells express numerous integrin receptors (36). Of these, *ITGA3*, *ITGA6*, *ITGA8* and *ITGB1* were significantly downregulated at various points in the time scale. All are involved in cell attachment to collagen and other substrate adhesion molecules and function to provide cell-matrix linkage. Integrin $\alpha3\beta1$ is one of the integrin heterodimers that binds to type I collagen, while the adhesion of fibroblastic cells to laminin is mediated by both $\alpha3\beta1$ and $\alpha6\beta1$ integrins (37). Integrin $\alpha8$ also forms heterodimers with integrin $\beta1$ and functions as a receptor for tenascin, fibronectin and vitronectin (38). Reduction in the expression of these genes is therefore consistent with detachment and reorientation of the cells observed microscopically, as was downregulation in the expression of the *NCAM1* and *VTN* genes.

The next puzzle is how this might be mediated. Members of the MMP family of proteolytic enzymes are the most likely candidates. Sixteen members of the MMP family were constitutively expressed at C_t values < 35 , including seven MMPs, three membrane type matrix metalloproteinases (MT-MMPs), three a disintegrin and metalloproteinases with thrombospondin motifs (ADAMTSs) and three TIMPs. TIMPs are important extracellular regulators of MMPs, and numerous studies suggest that pathophysiological resorption is correlated with an

Table 2. Alterations in the expression of adhesion-related genes by human periodontal ligament cells following cyclic mechanical strain

Name of gene	Description	Fold up- or downregulation (experimental/control)					
		6 h	<i>p</i> -Value	12 h	<i>p</i> -Value	24 h	<i>p</i> -Value
<i>ADAMTS1</i>	Metallopeptidase thrombospondin I motif 1	1.29	0.0066	1.11	0.3452	1.32	0.0226
<i>ADAMTS13</i>	Metallopeptidase thrombospondin I motif 13	-1.53	0.3163	1.28	0.4690	-1.81	0.2037
<i>ADAMTS8</i>	Metallopeptidase thrombospondin I motif 8	1.04	0.9293	-1.07	0.8240	1.48	0.5384
<i>CD44</i>	CD44 molecule	1.03	0.6003	1.06	0.3214	1.05	0.1468
<i>CDH1</i>	Cadherin 1, type 1, E-cadherin (epithelial)	ND	ND	ND	ND	ND	ND
<i>CLEC3B</i>	C-type lectin domain family 3, member B	1.02	0.8951	-1.13	0.7379	1.12	0.6066
<i>CNTN1</i>	Contactin 1	-1.04	0.8663	-1.15	0.5570	-1.41	0.0926
<i>COL1A1</i>	Collagen, type I, α 1	-1.08	0.4576	-1.04	0.9074	1.02	0.8773
<i>COL4A2</i>	Collagen, type IV, α 2	1.04	0.7795	1.06	0.7367	-1.04	0.6374
<i>COL5A1</i>	Collagen, type V, α 1	-1.01	0.9314	-1.19	0.3741	1.15	0.3449
<i>COL6A1</i>	Collagen, type VI, α 1	-1.06	0.5398	-1.64	0.0425	1.06	0.6791
<i>COL6A2</i>	Collagen, type VI, α 2	-1.11	0.2276	-1.44	0.1504	-1.14	0.5632
<i>COL7A1</i>	Collagen, type VII, α 1	-1.03	0.8950	1.13	0.6816	1.10	0.7741
<i>COL8A1</i>	Collagen, type VIII, α 1	-1.19	0.3865	-1.35	0.0165	-1.28	0.2641
<i>COL11A1</i>	Collagen, type XI, α 1	1.03	0.9373	1.13	0.4348	-2.49	0.0169
<i>COL12A1</i>	Collagen, type XII, α 1	-1.18	0.5391	-1.21	0.6089	-1.14	0.2274
<i>COL14A1</i>	Collagen, type XIV, α 1	-1.37	0.1790	1.07	0.4394	-1.01	0.9558
<i>COL15A1</i>	Collagen, type XV, α 1	-1.06	0.7353	-1.20	0.6717	1.09	0.3297
<i>COL16A1</i>	Collagen, type XVI, α 1	-1.09	0.3610	-1.07	0.5466	1.01	0.9213
<i>CTGF</i>	Connective tissue growth factor	-1.29	0.1011	-1.26	0.3554	1.36	0.0156
<i>CTNNA1</i>	Catenin (cadherin-associated protein), α 1	1.06	0.7314	-1.61	0.1544	-1.03	0.5492
<i>CTNNB1</i>	Catenin (cadherin-associated protein), β 1	-1.13	0.2498	-1.13	0.3472	-1.08	0.1917
<i>CTNND1</i>	Catenin (cadherin-associated protein), δ 1	1.02	0.8601	-1.66	0.1624	-1.05	0.4233
<i>CTNND2</i>	Catenin (cadherin-associated protein), δ 2	-1.02	0.9193	1.02	0.8303	-1.30	0.3117
<i>ECM1</i>	Extracellular matrix protein 1	-1.03	0.6846	-1.04	0.7175	-1.04	0.4154
<i>FN1</i>	Fibronectin 1	-1.09	0.5283	1.27	0.1587	1.10	0.4764
<i>HAS1</i>	Hyaluronan synthase 1	-1.01	0.9887	ND	ND	-2.34	0.1135
<i>ICAM1</i>	Intercellular adhesion molecule 1 (CD54)	1.62	0.1396	1.74	0.0262	1.00	0.9986
<i>ITGA1</i>	Integrin, α 1	-1.17	0.2650	-1.32	0.1899	-1.27	0.1350
<i>ITGA2</i>	Integrin, α 2	-1.03	0.8958	-1.69	0.1760	-1.20	0.3546
<i>ITGA3</i>	Integrin, α 3	1.03	0.8138	-1.22	0.0469	-1.09	0.6196
<i>ITGA4</i>	Integrin, α 4	-1.05	0.7425	-1.13	0.6331	-1.19	0.2664
<i>ITGA5</i>	Integrin, α 5	1.01	0.8561	-1.05	0.5481	1.17	0.2033
<i>ITGA6</i>	Integrin, α 6	-1.16	0.1839	-1.11	0.6650	-1.23	0.0283
<i>ITGA7</i>	Integrin, α 7	-1.13	0.4213	1.01	0.9716	-1.06	0.7357
<i>ITGA8</i>	Integrin, α 8	-1.14	0.0157	-1.25	0.0348	1.23	0.3822
<i>ITGAL</i>	Integrin, α L	ND	ND	ND	ND	ND	ND
<i>ITGAM</i>	Integrin, α M	ND	ND	ND	ND	ND	ND
<i>ITGAV</i>	Integrin, α V	-1.14	0.4016	-1.03	0.8566	-1.14	0.1614
<i>ITGB1</i>	Integrin, β 1	-1.30	0.6177	-1.18	0.0367	-1.03	0.7270
<i>ITGB2</i>	Integrin, β 2	-1.15	0.4842	1.28	0.1568	1.00	0.9833
<i>ITGB3</i>	Integrin, β 3	1.06	0.9117	-1.65	0.5671	-1.71	0.1364
<i>ITGB4</i>	Integrin, β 4	-1.31	0.3184	-1.15	0.5688	-2.25	0.1559
<i>ITGB5</i>	Integrin, β 5	-1.02	0.8581	-1.07	0.1374	1.09	0.1953
<i>KAL1</i>	Kallmann syndrome 1 sequence	ND	ND	ND	ND	ND	ND
<i>LAMA1</i>	Laminin, α 1	1.08	0.5504	-1.06	0.7369	1.01	0.8778
<i>LAMA2</i>	Laminin, α 2	4.77	0.4376	-1.31	0.2733	-1.16	0.3614
<i>LAMA3</i>	Laminin, α 3	-1.13	0.4386	-1.16	0.0702	-1.07	0.7036
<i>LAMB1</i>	Laminin, β 1	-1.17	0.3092	-1.06	0.3932	-1.10	0.2048
<i>LAMB3</i>	Laminin, β 3	-1.05	0.5515	-1.23	0.1162	-1.16	0.2154
<i>LAMC1</i>	Laminin, γ 1 (formerly <i>LAMB2</i>)	-1.03	0.8356	-1.40	0.2434	-1.20	0.1382
<i>MMP1</i>	Matrix metalloproteinase 1	1.08	0.5536	ND	ND	1.03	0.5905
<i>MMP2</i>	Matrix metalloproteinase 2	-1.10	0.3379	-1.04	0.6927	-1.08	0.4806
<i>MMP3</i>	Matrix metalloproteinase 3	-1.03	0.7509	1.30	0.0759	-1.29	0.0609
<i>MMP7</i>	Matrix metalloproteinase 7	ND	ND	ND	ND	ND	ND
<i>MMP8</i>	Matrix metalloproteinase 8	-1.33	0.0788	-1.21	0.5606	-2.02	0.0103
<i>MMP9</i>	Matrix metalloproteinase 9	ND	ND	ND	ND	ND	ND
<i>MMP10</i>	Matrix metalloproteinase 10	-1.21	0.2620	1.14	0.2692	1.03	0.8722
<i>MMP11</i>	Matrix metalloproteinase 11	-1.23	0.1800	-1.35	0.0364	-1.09	0.5464
<i>MMP12</i>	Matrix metalloproteinase 12	-1.13	0.4218	1.20	0.1692	-1.16	0.3762

Table 2.(Continued)

Name of gene	Description	Fold up- or downregulation (experimental/control)					
		6 h	p-Value	12 h	p-Value	24 h	p-Value
<i>MMP13</i>	Matrix metalloproteinase 13	ND	ND	ND	ND	ND	ND
<i>MMP14</i>	Matrix metalloproteinase 14	1.01	0.9360	-1.22	0.1830	1.11	0.4988
<i>MMP15</i>	Matrix metalloproteinase 15	-1.92	0.0077	1.54	0.2398	ND	ND
<i>MMP16</i>	Matrix metalloproteinase 16	-1.04	0.8018	-1.07	0.6069	-1.16	0.1985
<i>NCAM1</i>	Neural cell adhesion molecule 1	-1.09	0.0268	-1.31	0.3457	1.22	0.0535
<i>PECAM1</i>	Platelet/endothelial cell adhesion molecule	1.23	0.6156	-1.11	0.8371	ND	ND
<i>SELE</i>	Selectin E (endothelial adhesion molecule 1)	ND	ND	ND	ND	ND	ND
<i>SELL</i>	Selectin L (lymphocyte adhesion molecule 1)	ND	ND	ND	ND	ND	ND
<i>SELP</i>	Selectin P	ND	ND	ND	ND	ND	ND
<i>SGCE</i>	Sarcoglycan, ϵ	ND	ND	ND	ND	ND	ND
<i>SPARC</i>	Secreted protein, acidic, cysteine-rich	-1.06	0.4308	1.08	0.5330	1.16	0.2112
<i>SPG7</i>	Spastic paraplegia 7	1.00	0.9901	1.06	0.6940	-1.24	0.5028
<i>SPP1</i>	Secreted phosphoprotein 1	1.12	0.4623	1.76	0.0037	1.08	0.4308
<i>TGFBI</i>	Transforming growth factor, β 1	-1.07	0.6058	-1.42	0.2495	-1.06	0.5762
<i>THBS1</i>	Thrombospondin 1	1.03	0.8460	-1.00	0.9998	-1.06	0.0916
<i>THBS2</i>	Thrombospondin 2	-1.06	0.7065	-1.13	0.1886	-1.38	0.1202
<i>THBS3</i>	Thrombospondin 3	-1.16	0.3227	-1.00	0.9994	-1.07	0.6746
<i>TIMP1</i>	TIMP metalloproteinase inhibitor 1	-1.04	0.8334	1.46	0.3405	1.29	0.1863
<i>TIMP2</i>	TIMP metalloproteinase inhibitor 2	-1.06	0.5450	-1.22	0.1819	-1.07	0.5713
<i>TIMP3</i>	TIMP metalloproteinase inhibitor 3	1.45	0.4867	-2.41	0.2673	ND	ND
<i>TNC</i>	Tenascin C (hexabrachion)	-1.00	0.9796	1.62	0.0853	1.37	0.1043
<i>VCAM1</i>	Vascular cell adhesion molecule 1	-1.48	0.0619	-1.08	0.8198	1.16	0.6055
<i>VCAN</i>	Versican	-1.08	0.8172	-1.23	0.7692	-1.32	0.2985
<i>VTN</i>	Vitronectin	-1.78	0.0051	1.26	0.6872	-1.70	0.0995
Calibrator genes							
<i>B2M</i>	β 2-Microglobulin	-1.11	0.1353	-1.02	0.7025	-1.10	0.4223
<i>HPRT1</i>	Hypoxanthine phosphoribosyltransferase 1	-1.05	0.4378	-1.02	0.9281	-1.07	0.3070
<i>RPL13A</i>	Ribosomal protein L13A	1.07	0.3091	1.15	0.2733	-1.02	0.8371
<i>GAPDH</i>	Glyceraldehyde-3-phosphate dehydrogenase	1.04	0.5191	-1.25	0.2964	1.19	0.0824
<i>ACTB</i>	Actin, β	1.05	0.0990	1.13	0.1943	1.01	0.8100

A grey box indicates a statistically significant change ($*p < 0.05$). ND, not detected.

imbalance of inhibitors and proteinases (39). Many biological processes have been linked to these enzymes, but given the similarities in the functional domains of MMPs, MT-MMPs and ADAMTSs and the fact they are all inhibited by TIMPs to varying degrees, considerable potential exists for functional redundancy in their biological activities. Four members of the MMP family showed significant alterations in expression; *MMP8* (neutrophil collagenase), *MMP11* (stromelysin-3) and *MMP15* (MT2-MMP) were all downregulated, while *ADAMTS1* was upregulated. The upregulation of *ADAMTS1* at 6 and 24 h suggests an important role for this enzyme in mechanically induced matrix remodeling, and of interest in this regard is the finding that parathyroid hormone stimulates *ADAMTS1* synthesis and

collagen degradation by human osteoblasts in culture (40). Both *TIMP1* and *TIMP2* were expressed at high copy numbers, but were not responsive to mechanical deformation.

Of the twelve genes encoding collagen α -chains that were constitutively expressed, three were significantly downregulated, the short-chain collagens *COL6A1* and *COL8A1* at 12 h and *COL11A1* at 24 h. We have previously reported that cyclic tensile strain downregulates *COL3A1* and *COL11A1* expression (6). Collagen type VI is a ubiquitous extracellular matrix protein, which forms microfibrillar networks with other matrix proteins (41,42), while collagen type -VIII is a nonfibrillar collagen present in a variety of extracellular matrices, including basement membranes (43). Although the function of these colla-

gens is not well understood, their binding activity suggests that they have an anchoring function and play a role in cell migration and differentiation.

Although not a cell-adhesion factor, CTGF, which functions as a growth factor for fibroblasts and other connective tissue cells (44), was included in the gene array. Connective tissue growth factor is mitogenic and chemotactic for fibroblasts and is selectively induced by transforming growth factor- β (TGF- β ; 45), and its role as a downstream mediator of TGF- β signalling has led to it being widely studied in wound repair and various types of fibrotic disease (46). Most recently, CTGF has been shown to direct fibroblast differentiation from periodontal ligament progenitor cells (47) and human mesenchymal stem/stromal cells (48), which has implications for

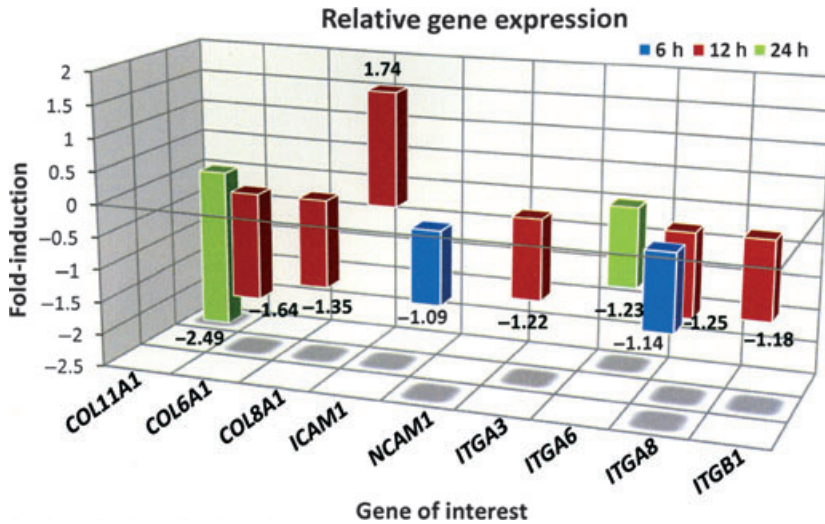


Fig. 3. Fold-induction (C_t ratio) of nine genes showing a statistically significant ($p < 0.05$) change in mRNA expression in response to a uniaxial, cyclic tensile strain of 12%, three coding collagen α -chains, two cell-adhesion molecules and four integrin subunits. All were downregulated, with the exception of the transmembrane protein *ICAM1*, which was upregulated 1.74-fold.

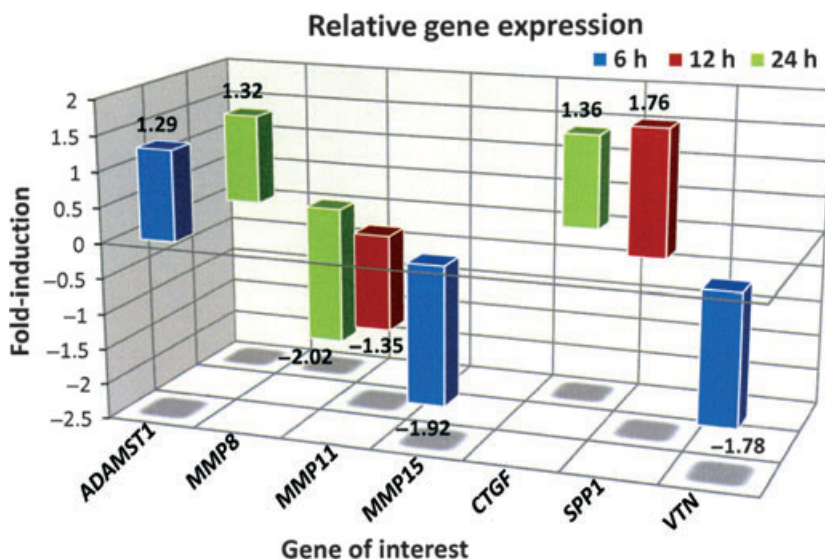


Fig. 4. Three-dimensional profile showing statistically significant alterations ($p < 0.05$) in mRNA expression (C_t ratio) of the following seven genes encoding four members of the MMP family of proteolytic enzymes: the fibroblast differentiation gene, *CTGF*, and the extracellular matrix proteins, *SPP1* (osteopontin) and *VTN*. *ADAMST1* was one of only two genes altered across two time points.

the present study. The increase in *CTGF* expression together with upregulation of the genes for two TGF- β isoforms (*TGF β 1* and *TGF β 3*) in the same model system (8) is strongly indicative of a causal relationship, and suggests that *CTGF* functions in the periodontal ligament to maintain the fibroblast phenotype.

Previous studies of the effect of mechanical strain on gene expression by periodontal ligament cells have been referenced against a single calibrator or housekeeping gene, most commonly *GAPDH* or *ACTB*. By measuring expression profiles relative to the mean C_t values of five different calibrator genes (Table 1), the present methodol-

ogy represents an important advance. Ideally, the experimental conditions should not influence the expression of the calibrator gene, but calibrator gene expression is invariably affected by the experimental conditions (49). If validation data do exist, calibrator genes should be selected on the basis of their predicted stability in specific experimental conditions, because currently there is no calibrator gene that is stable in every system, in every circumstance and for every cell type (50). In other words, because an all-purpose calibrator gene does not exist, accurate normalization of real-time RT-PCR data can only be achieved by averaging multiple calibrator gene expression (51,52). Another advantage of the experimental design is that by measuring the samples in triplicate, it is possible to obtain more statistically robust data than obtainable by using a treated/control ratio of ± 2 as representing significant change. The present study indicates that use of the latter will result in a considerable number of false negatives as well as some false positives; of the fifteen genes recording a statistically significant change in expression, for the majority ($n = 13$) the C_t ratio was < 2 .

In conclusion, this investigation has demonstrated a complex set of interactions between human periodontal ligament cells cultured *in vitro* and a mechanically active two-dimensional collagen substrate. The C_t ratios may seem modest, but the alterations in relative expression represent averages over the entire strain field, where the magnitude and type of strain experienced will vary depending on the location of the cells within the field. Nevertheless, alterations in the pattern of expression are suggestive of a homeostatic mechanism whereby cell adhesion molecules are predominately downregulated to facilitate cellular reorientation in response to their altered functional environment. Some of these genes are also involved in cellular mechanosensing, and changes in their pattern of expression carry implications for the activation of a number of downstream mechanotransduction pathways.

Nevertheless, additional studies will be necessary to establish whether the

expressed genes are translated into protein and, if they are, whether they are biologically active. This will require assaying culture supernatants for the expressed proteins of interest and immunolocalization of the proteins *in situ* with specific antibodies in animal models of tooth movement. Another consideration is that the traditional two-dimensional culture systems in widespread use for investigating the response of cells to mechanical strain *in vitro* have a number of limitations, not least the fact that periodontal ligament cells are normally surrounded by a complex network of collagens, proteoglycans and noncollagenous proteins, which are not grown on tissue culture plastic or films of matrix proteins, such as collagen or fibronectin. Some attempt has been made to address this shortcoming for compressive force application by seeding periodontal ligament cells into type I collagen gels (4,5), but collagen is only one of the major structural macromolecules found in extracellular matrices. For the field to progress, therefore, it is clear that future *in vitro* analyses of mechanoresponsive gene and protein expression require well-characterized three-dimensional models incorporating periodontal ligament cells into hydrogel matrices designed to produce a tissue construct resembling more closely the periodontal ligament *in vivo*.

Acknowledgements

We are grateful for financial support from the National University of Singapore Academic Research Fund (R222-000-029-112), the New Zealand Lottery Grants Board, NZ Dental Association Research Foundation, NZ Association of Orthodontists, and the University of Otago Research Committee.

References

- Shimizu N, Yamaguchi M, Goseki T *et al*. Cyclic-tension force stimulates interleukin-1 β production by human periodontal ligament cells. *J Periodont Res* 1994;**29**: 328–333.
- Long P, Hu J, Piesco N, Buckley M, Agarwal S. Low magnitude of tensile strain inhibits IL-1 β -dependent induction of pro-inflammatory cytokines and induces synthesis of IL-10 in human periodontal ligament cells *in vitro*. *J Dent Res* 2001;**80**:1416–1420.
- Kanzaki H, Chiba M, Shimizu Y, Mitani H. Periodontal ligament cells under mechanical stress induces osteoclastogenesis by receptor activator of nuclear factor κ B ligand up-regulation via prostaglandin E₂ synthesis. *J Bone Miner Res* 2002;**17**:210–220.
- Lee Y-H, Nahm D-S, Jung Y-K *et al*. Differential gene expression of periodontal ligament cells after loading of static compressive force. *J Periodontol* 2007;**78**: 446–452.
- de Araujo RMS, Oba Y, Moriyama K. Identification of genes related to mechanical stress in human periodontal ligament cells using microarray analysis. *J Periodont Res* 2007;**42**:15–22.
- Wescott DC, Pinkerton MN, Gaffey BJ, Beggs KT, Milne TJ, Meikle MC. Osteogenic gene expression by human periodontal ligament cells under cyclic tension. *J Dent Res* 2007;**86**:1212–1216.
- Yamashiro K, Myokai F, Hiratsuka K *et al*. Oligonucleotide array analysis of cyclic tension-responsive genes in human periodontal ligament fibroblasts. *Int J Biochem Cell Biol* 2007;**39**: 910–921.
- Pinkerton MN, Wescott DC, Gaffey BJ, Beggs KT, Milne TJ, Meikle MC. Cultured human periodontal ligament cells constitutively express multiple osteotropic cytokines and growth factors, several of which are responsive to mechanical deformation. *J Periodont Res* 2008;**43**: 343–351.
- Wang N, Butler JP, Ingber DE. Mechanotransduction across the cell surface and through the cytoskeleton. *Science* 1993;**269**:1124–1127.
- Clarke EA, Brugge JS. Integrins and signal transduction pathways: the road taken. *Science* 1995;**268**:233–239.
- Sastry SK, Burrige K. Focal adhesions: a nexus for intracellular signaling and cytoskeletal dynamics. *Exp Cell Res* 2000;**261**:25–36.
- Wyllie AH, Kerr JFR, Currie AR. Cell death: the significance of apoptosis. *Int Rev Cytol* 1980;**68**:251–307.
- Elmore S. Apoptosis: a review of programmed cell death. *Toxicol Pathol* 2007;**35**:495–516.
- Bakker A, Klein-Nulend J, Burger E. Shear stress inhibits while disuse promotes osteocyte apoptosis. *Biochem Biophys Res Commun* 2004;**320**:1163–1168.
- Aguirre JI, Plotkin LI, Stewart SA *et al*. Osteocyte apoptosis is induced by weightlessness in mice and precedes osteoclast recruitment and bone loss. *J Bone Miner Res* 2006;**21**:605–615.
- Zhong W, Xu C, Zhang F, Jiang X, Zhang X, Ye D. Cyclic stretching force-induced early apoptosis in human periodontal ligament cells. *Oral Dis* 2008;**14**:270–276.
- Hao Y, Xu C, Sun S, Zhang F. Cyclic stretching force induces apoptosis in human periodontal ligament cells via Caspase-9. *Arch Oral Biol* 2009;**54**: 864–870.
- Somerman MJ, Archer SY, Imm GR, Foster RA. A comparative study of human periodontal ligament cells and gingival fibroblasts *in vitro*. *J Dent Res* 1988;**67**:66–70.
- Natali AN, Pavan PG, Scarpa C. Numerical analysis of tooth mobility: formulation of a non-linear constitutive law for the periodontal ligament. *Dent Mater* 2004;**20**:623–629.
- Mosmann T. Rapid colorimetric assay for cellular growth and survival: application to proliferation and cytotoxicity assays. *J Immunol Methods* 1983;**65**:55–63.
- Twentyman PR, Luscombe M. A study of some variables in a tetrazolium dye (MTT) based for cell growth and chemosensitivity. *Br J Cancer* 1987;**56**:279–285.
- Chomczynski P, Sacchi N. Single-step method of RNA isolation by acid guanidinium thiocyanate-phenol-chloroform extraction. *Anal Biochem* 1987;**162**:156–159.
- Livak KJ, Schmittgen TD. Analysis of relative gene expression data using real-time quantitative PCR and the 2^{- $\Delta\Delta$ C(T)} method. *Methods* 2001;**25**:402–408.
- Yuan JS, Reed A, Chen F, Stewart CN. Statistical analysis of real-time PCR data. *BMC Bioinformatics* 2006;**7**:85–97.
- Buckley MJ, Banes AJ, Levin LG *et al*. Osteoblasts increase their rate of cell division and align in response to cyclic, mechanical tension *in vitro*. *Bone Miner* 1988;**4**:225–236.
- Neidlinger-Wilke C, Grood E, Claes L, Brand R. Fibroblast orientation to stretch begins within three hours. *J Orthop Res* 2002;**20**:953–956.
- Matheson LA, Fairbank NJ, Maksym GN, Santerre JP, Labow RS. Characterization of the FlexcellTM cyclic strain culture system with U937 macrophage-like cells. *Biomaterials* 2006;**27**:226–233.
- Vande Geeste JP, Di Martino ES, Vorp DA. An analysis of the complete strain field within FlexercellTM membranes. *J Biomech* 2004;**37**:1923–1928.
- Wall ME, Weinholt PS, Siu T, Brown TD, Banes AJ. Comparison of cellular strain with applied substrate strain *in vitro*. *J Biomech* 2007;**40**:173–181.
- Milne TJ, Ichim I, Patel B, McNaughton A, Meikle MC. Induction of osteopenia during experimental tooth movement in the rat: alveolar bone remodelling and the mechanostat theory. *Eur J Orthodont* 2009;**31**:221–231.

31. Wang Y, Li Y, Fan X, Zhang Y, Wu J, Zhao Z. Early proliferation alteration and differential expression in human periodontal ligament cells subjected to cyclic tensile stress. *Arch Oral Biol* 2011;**56**:177–186.
32. Danciu TE, Gagari E, Adam RM, Damoulis PD, Freeman MR. Mechanical strain delivers anti-apoptotic and proliferative signals to gingival fibroblasts. *J Dent Res* 2004;**83**:596–601.
33. Boccafoschi F, Sabbatini M, Bosetti M, Cannas M. Overstressed mechanical stretching activates survival and apoptotic signals in fibroblasts. *Cells Tissues Organs* 2010;**192**:167–176.
34. Boccafoschi F, Bosetti M, Gatti S, Cannas M. Dynamic fibroblast cultures: response to mechanical stretching. *Cell Adh Migr* 2007;**1**:124–128.
35. Meyer CJ, Alenghat FJ, Rim P, Fong JH, Fabry B, Ingber DE. Mechanical control of cyclic AMP signaling and gene transcription through integrins. *Nat Cell Biol* 2000;**2**:666–668.
36. Lallier TE, Yukna R, Moses RL. Extracellular matrix molecules improve periodontal ligament cell adhesion to anorganic bone matrix. *J Dent Res* 2001;**80**:1748–1752.
37. Kikkawa Y, Sanzen N, Fujiwara H, Sonnenberg A, Sekiguchi K. Integrin binding specificity of laminin-10/11: laminin-10/11 are recognized by $\alpha 3\beta 1$, $\alpha 6\beta 1$ and $\alpha 6\beta 4$ integrins. *J Cell Sci* 2000;**113**:859–876.
38. Schnapp LM, Hatch N, Ramos DM, Klimanskaya IV, Sheppard D, Pytela R. The human integrin $\alpha 8\beta 1$ functions as a receptor for tenascin, fibronectin and vitronectin. *J Biol Chem* 1995;**270**:23196–23202.
39. Murphy G, Reynolds JJ. Extracellular matrix degradation. In: Royce PM, Steinmann B, eds. *Connective Tissue and Its Heritable Disorders*. New York: Wiley-Liss Inc, 1993:287–316.
40. Rehn AP, Birch MA, Karlström E, Wendel M, Lind T. ADAMTS-1 increases the three-dimensional growth of osteoblasts through type I collagen processing. *Bone* 2007;**41**:231–238.
41. Engel J, Furthmayr H, Odermatt E *et al*. Structure and macromolecular organization of type VI collagen. *Ann N Y Acad Sci* 1985;**460**:25–37.
42. Lampe AK, Bushby KMD. Collagen VI related muscle disorders. *J Med Genet* 2005;**42**:673–685.
43. Shuttleworth CA. Type VIII collagen. *Int J Biochem Cell Biol* 1997;**29**:1145–1148.
44. Igarashi A, Okochi H, Bradham DM, Grotendorst GR. Regulation of connective tissue growth factor gene expression in human skin fibroblasts and during wound repair. *Mol Biol Cell* 1993;**4**:637–645.
45. Kothapalli D, Frazier KS, Welphy A, Segarini PR, Grotendorst GR. Transforming growth factor b induces anchorage-independent growth of NRK fibroblasts via a connective tissue growth factor-independent signaling pathway. *Cell Growth Differ* 1997;**8**:61–68.
46. Werner S, Grose R. Regulation of wound healing by growth factors and cytokines. *Physiol Rev* 2003;**83**:835–870.
47. Dangaria SJ, Ito Y, Walker C, Druzinsky R, Luan X, Diekwisch TGH. Extracellular matrix-mediated differentiation of periodontal progenitor cells. *Differentiation* 2009;**78**:79–90.
48. Lee CH, Shah B, Moiola EK, Mao JJ. CTGF directs fibroblast differentiation from human mesenchymal stem/stromal cells and defines connective tissue healing in a rodent injury model. *J Clin Invest* 2010;**120**:3340–3349.
49. Schmittgen TD, Zakrajsek BA. Effect of experimental treatment on housekeeping gene expression: validation by real-time, quantitative RT-PCR. *J Biochem Biophys Methods* 2000;**46**:69–81.
50. Farrel R. *RNA Methodologies. A Laboratory Guide for Isolation and Characterization*. Burlington: Elsevier Academic Press, 2005.
51. Vandesompele J, De Preter K, Pattyn F *et al*. Accurate normalization of real-time quantitative RT-PCR data by geometric averaging of multiple internal control genes. *Genome Biol* 2002;**3**: research 0034.1–0034.11.
52. Dheda K, Huggett JF, Chang JS *et al*. The implications of using an inappropriate reference gene for real-time reverse transcription PCR data normalization. *Anal Biochem* 2005;**344**:141–143.

This document is a scanned copy of a printed document. No warranty is given about the accuracy of the copy. Users should refer to the original published version of the material.